A Rain and Scintillation Ka-band Channel Simulator

J. Sala, M. Lamarca, J. A. López, F. Rey, J. Riba, G. Vázquez, X. Villares
A. M. Jalón(#), P. Rodríguez(#)
Dpt. of Signal Theory and Communications, Technical University of Catalonia
c/Jordi Girona 1-3, Campus Nord UPC, D5-114b, 08034 Barcelona, SPAIN
E-mail: josep.sala@upc.edu, WWW: http://gps-tsc.upc.es/comm
(#)Thales Alenia Space España (TAS-E), c/ Einstein 7, PTM 28760 Tres Cantos, Madrid
E-mail: a.jalon@thalesaleniaspace.com

Abstract— **This paper describes the implementation of a Ka-band satellite channel simulator with emphasis on the synthesis of scintillation processes. The problem becomes one of generating a given probability density function, the Moulsley-Vilar distribution, with a specified power spectral density using a Wiener model based on orthogonal Hermite polynomials for the nonlinearity. A numerical procedure is devised to calculate the filter and non-linearity coefficients of the Wiener model. The generation of rain processes conforms to the Maseng-Bakken model.**

I. Introduction

The saturation of current satellite bands and the increasing demand for broadband satellite services has led to considering the Ka-band (18-30 GHz), where propagation is subject to slowly time-varying attenuation. Adaptive Coding and Modulation (ACM) is used for matching the transmission rate to the instantaneous channel conditions so that this slow variation in the channel attenuation ultimately affects the global average (ergodic) rate to the user population over a sufficiently long time period. The availability of Channel State Information (CSI), expressed in terms of the received Signal-to-Noise Ratio (SNR), allows to select the most appropriate modulation and coding rate for each user via the ACM control loop.

The tropospheric propagation channel conforms to a Frequency Flat Fading (FFF) model, whose time-varying attenuation is the combination of two effects: (i) attenuation by hydro-meteors, characterized by the Maseng-Bakken model [1]; (ii) scintillation, turbulent tropospheric refraction due to random variations of the refractive index [2]. Both a static and a dynamic model are required for characterizing attenuation induced by rain and scintillation. In the former, the Probability Density Function (PDF) of the attenuation (dB) of both effects have been found experimentally: the log-normal and Moulsley-Vilar (MV) distributions [3] for rain and scintillation, respectively. In the latter, the Power Spectral Density (PSD) of the attenuation process is specified. The stochastic dynamic model of rain attenuation considers a scheme for generating the log-normal distribution of attenuation with a specified power spectral density, with bandwidths in the milli-Hertz range and potentially large attenuation events. Scintillation is characterized instead by small (tenths of dB) attenuation and relatively fast variations (typically in the Hz range).

The ACM control loop is mainly driven by rain attenuation (slow variation) while scintillation is present as relatively fast and small variations with respect to the present value of rain attenuation. The ACM loop settings (SNR thresholds between different modulation and coding schemes) have to be adjusted to take scintillation into account: variations of 1 dB at 30 GHz may be typical of scintillation [4], which lead to an order of magnitude increase in the short-term Bit-Error Rate (BER).

Testbenches for the evaluation of Fading Mitigation Techniques (FMT), as carried out in [5], require a satellite channel simulator which models the described FFF effects. As rain synthesis is fully specified in the Maseng-Bakken model, we will consider a Wiener model for the synthesis of scintillation in the channel simulator.

II. Characterization of Scintillation

The MV distribution refers to scintillation attenuation expressed in dB. Theoretical models of the scintillation

[1]This work has been financed by ESA/ESTEC project "Adaptive DVB-RCS1/DVB-S2 On-Board Processing (OBP) for Broadband Meshed Communications", the Spanish Government TEC2007-68094-C02-2, and the DURSI/ Catalan Government Grant 2005SGR-00639 .

978-1-4244-2573-0/08/$25.00 ©2008 IEEE

PSD have been derived, although they match experimental data only partially. In this work, we provide a synthesis method that conforms to the static and dynamic characterization of scintillation. The MV PDF of the scintillation process χ conditioned to a given standard deviation σ_χ is expressed from a Gaussian density as,

$$p(\chi|\sigma_\chi) = \frac{1}{\sqrt{2\pi}\sigma_\chi} \cdot e^{-\chi^2/2\sigma_\chi^2} \quad (1)$$

where σ_χ^2 is itself a log-normally distributed random variable. The probability density of its standard deviation σ_χ becomes,

$$p_\sigma(\sigma_\chi) = \sqrt{\frac{2}{\pi}} \cdot \frac{1}{\sigma_\chi \sigma_\sigma} \cdot \exp\left(-\frac{\ln^2(\sigma_\chi^2/\sigma_m^2)}{2\sigma_\sigma^2}\right)$$

with σ_m and σ_σ the parameters which control the mean level and spread of the standard deviation σ_χ of scintillation, respectively. The *peaky* appearance of scintillation is governed by the ratio σ_σ/σ_m. The exact expression of the MV distribution cannot be calculated explicitly, although approximations have been reported. It is given by the following marginalization,

$$p_X(\chi) = \int_0^{+\infty} p(\chi|\sigma_\chi) p_\sigma(\sigma_\chi) d\sigma_\chi \quad (2)$$

The PSD of scintillation has also been measured in experimental campaigns and theoretical studies exist that predict a spectral index of $-8/3$ from Turbulence Theory [2][7] which has been verified experimentally, at least within a band of the total scintillation spectrum. Therefore, we have used the following approximation to the true scintillation PSD,

$$S_{\chi\chi}(f) = S_0 \cdot \frac{1}{1 + (f/f_\chi)^\nu} \quad (3)$$

with $\nu = 8/3$ and S_0 a normalization term.

III. The Wiener Model

We consider a Wiener model (filter followed by non-linearity) fed with white Gaussian noise for the generation of scintillation, according to the scheme depicted in figure (1). The synthesis of Gaussian processes with a specified PSD from white Gaussian noise can be done with a synthesis filter as this operation does not alter Gaussianity. Nevertheless, when we intend to generate a non-Gaussian PDF such as that of scintillation with a pre-specified PSD, the nonlinearity modifies the PSD of the input process. Hence, the computation of the filter and non-linearity coefficients are coupled.

Previous results [6] can be used to solve this problem. Let $F_X(x)$ and $F_N(x)$ denote the target and normal cumulative distributions, respectively. Then, the nonlinearity that synthesizes the target distribution from normal Gaussian noise is given by $g(x) = F_X^{-1}(F_N(x))$, with $F_X^{-1}(x)$ the inverse function of the target distribution such that $F_X(F_X^{-1}(x)) = x$. An expansion based on Hermite polynomials $H_k(x)$ is used to express $g(x)$,

$$g(x) = \sum_{k=-\infty}^{+\infty} g_k H_k(x) \quad (4)$$

with $H_n(x) = (-1)^n e^{x^2/2} \frac{\mathrm{d}^n}{\mathrm{d}x^n} e^{-x^2/2}$ and orthogonal with respect to the scalar product $< f(x), g(x) >= \int_{-\infty}^{+\infty} e^{-x^2/2} f(x) g(x) dx$. Therefore, the coefficients of the expansion are easily calculated from the following expectation with respect to N,

$$g_k = \frac{1}{k!} \cdot \mathbb{E}_N[g(N) H_k(N)] \quad (5)$$

with N a normal random variable: $p_N(n) = \frac{1}{\sqrt{2\pi}} \exp(-n^2/2)$. The relationship between the (unknown) input an (known) output correlation functions of $g(x)$ is expressed as,

$$\rho_{XX}[m] = \sum_{i=0}^{+\infty} b_i \cdot \rho_{CC}^i[m] \quad (6)$$

with $\rho_{CC}[m]$ and $\rho_{XX}[m]$ the m-th lag input and output correlations, respectively, and $b_i = i! g_i^2$. Therefore, Hermite polynomials allow to decouple the multivariate non-linear equation system into a set of univariate non-linear equations. If the target process can be synthesized by a Wiener model, this procedure will generate the required parameters.

IV. Numerical Procedure

In the implementation, we will use an approximation $\hat{g}(x)$ to the true $g(x)$. This will be based on a finite power expansion $\hat{g}(x) = \sum_{k=0}^{L} a_k \cdot x^k$, where due to the even symmetry of the MV PDF, only odd powers of x need be considered. The coefficients a_k will be calculated to minimize a cost function by polynomial regression on $g(x)$ using a suitable kernel $K(x)$. The choice of the kernel is critical to minimize the impact of large, low-probability values on the estimated coefficients.

The inverse Moulsley-Vilar cumulative distribution $F_X^{-1}(x)$ cannot be calculated explicitly. Nevertheless, if a sufficiently long data record $\mathbf{x}$ drawn according to this distribution is available, sorting provides a sufficiently accurate estimate of $F_X^{-1}(x)$ (for an infinitely long data record, the profile of sorted data converges to $F_X^{-1}(x)$). Evaluating,

$$\hat{F}_X^{-1}(x) = \mathrm{sort}[\mathbf{x}] \quad (7)$$

Fig. 1. Scintillation generation: a Random Number Generator (RNG) based on a bank a Linear Feedback Shift Registers (LFSR) feeds a White Gaussian Noise (WGN) generator, which is spectrally shaped by a linear discrete filter and passed through a memoryless nonlinearity $g(x)$.

we can derive the estimate $\hat{g}(x) = \hat{F}_X^{-1}(F_N(x))$, where the cumulative distribution of normal noise is,

$$F_N(x) \quad = \quad \frac{1}{2}\left(1 + \mathrm{erf}\left(\frac{x}{\sigma_g\sqrt{2}}\right)\right) \qquad (8)$$

with σ_g the standard deviation of Gaussian noise. The data input x to the sorting procedure must be drawn according to the MV distribution. Fortunately, we are only interested in estimating the inverse MV cumulative distribution without regard to its PSD. Hence, it only suffices to generate independent identically distributed samples. This is easily accomplished from the definition of the MV distribution, where normal Gaussian noise w is multiplied by an independent log-normal process s_χ. We may write,

$$x \quad = \quad w \cdot s_\chi \qquad (9)$$

The cost function for computing the unknown coefficients a_l is expressed in terms of a suitable kernel $K(x)$ as,

$$J \quad = \quad \frac{1}{M}\sum_{p=1}^{M} K(x_p) \cdot \left|\hat{g}(x_p) - \sum_l a_l \cdot x_p^{2l+1}\right|^2 \qquad (10)$$

Arranging the different powers x_p^{2l+1} into the data matrix $\mathbf{X}$, the coefficients a_l into the vector $\mathbf{a}$, the samples $\hat{g}(x_p)$ into vector $\mathbf{g}$ and the kernel values $K(x_p)$ into the diagonal matrix $\mathbf{K}$, we can express the cost function as,

$$J \quad = \quad (\hat{\mathbf{g}} - \mathbf{X}\mathbf{a})^{\mathrm{T}}\mathbf{K}(\hat{\mathbf{g}} - \mathbf{X}\mathbf{a}) \qquad (11)$$

from which we get the weighted least squares solution,

$$\mathbf{a}_{\mathrm{opt}} \quad = \quad (\mathbf{X}^{\mathrm{T}}\mathbf{K}\mathbf{X})^{-1}\mathbf{X}^{\mathrm{T}}\mathbf{K} \cdot \hat{\mathbf{g}} \qquad (12)$$

The high-order coefficients of $\mathbf{a}_{\mathrm{opt}}$ control the behaviour of the tails of the synthesized probability density. The kernel is responsible for controlling the effect of large and relatively fewer values of x_p, which has been chosen as,

$$K(x) \quad = \quad (1 + \mu \cdot x^\alpha)^{-1} \qquad (13)$$

where the exponent $\alpha = 2$ has proven to yield good experimental results.

Thereafter we get the autocorrelation values $\rho_{CC}[m]$ at the input to the non-linearity by solving the set of equations (6), an inverse prediction error filter is used to synthesize an approximation to the corresponding PSD using the Maximum Entropy Method (MEM) [8]. MEM will generate the *flattest* (highest entropy) PSD consistent with a finite number of known correlation lags $\rho_{CC}[m]$ (it extrapolates the autocorrelation sequence $\rho_{CC}[m]$ outside the known range).

V. Simulations

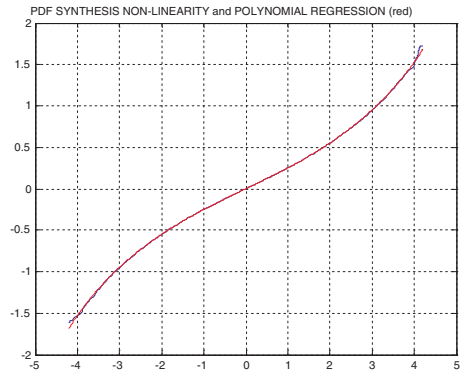

Fig. 2. Estimated Scintillation Non-Linearity: this odd non-linear function, of increasing derivative, generates the heavy-tailed distribution associated with scintillation on input a coloured Gaussian noise process as in figure (1).

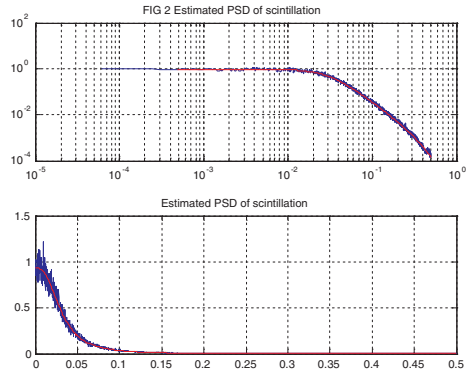

Fig. 3. Verification of synthesized scintillation Power Spectral Density (PSD) in double-logarithmic (above) and standard axes (below).

In the simulations we have used parameters gathered in the experimental campaigns of ACTS, Olympus and Italsat. Figure (3) compares the target and synthesized

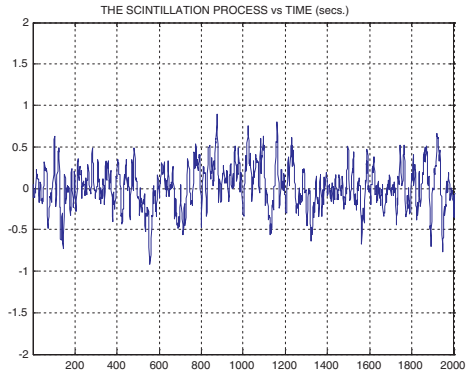

Fig. 4. Depiction of the scintillation process.

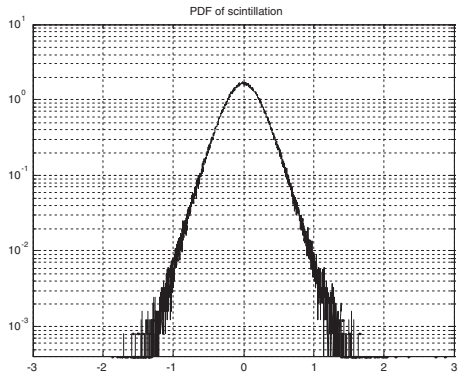

Fig. 5. Estimation (normalized histogram) of the probability density function of scintillation. The heavy tails can be observed in contrast to the parabolic shape of a Gaussian density.

PSD of a scintillation process, a random realization of scintillation appears in figure (4) and its corresponding PDF is shown in figure (5).

VI. Implementation

Representative scenarios for rain and scintillation have been defined for the testbench [5], incorporating several rain dynamics and independent weak/strong scintillation conditions. The corresponding parameters are precomputed and stored in the Channel Simulator (CS) for operation. Combinations of eight and four rain and scintillation scenarios, respectively, can be handled by the final prototype. Figure (6) shows the complete structure of the fading process generation. Both rain and scintillation are generated independently using a Wiener model (dry/wet scintillation can also be incorporated by modulating the scintillation process in terms of a nonlinear transformation of the rain process). Generation of rain and scintillation up to the output of nonlinearities $g(x)$ and $f(x)$ is performed at low rate. The output multistage interpolator increases the sampling rate to match that of the input communications signal. An exponential nonlinearity (not shown) performs the conversion of the total attenuation process to linear scale. Additive Gaussian Noise is added before the simulator output.

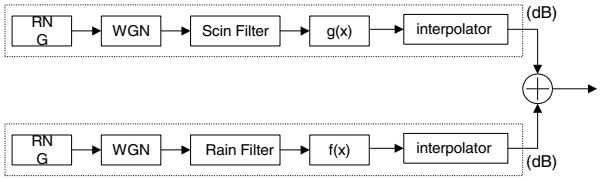

Fig. 6. Total rain plus scintillation generation at sampling rate.

The Channel Simulator has been implemented in a Xilinx Virtex II XC2V6000 FPGA. The package BF957 with a speed grade of -5 has been used, with a maximum 684 user I/Os.

The Channel simulator has taken up 6,250 Slice flip-flops (9% of the total in the FPGA), 21,377 4-input LUTs (31%). The total number of used slices is 12,762 (37%). The design has required 60 I/Os (23%), 12 internal Block RAMs (8%), 65 18x18-bit multipliers (45%) and 4 global clocks (25%). A total of 1,519,722 equivalent gates have been estimated for this design.

References

[1] Maseng, T.; Bakken, P.; "A Stochastic Dynamic Model of Rain Attenuation"; Communications, IEEE Transactions on [legacy, pre - 1988] Volume 29, Issue 5, May 1981 Page(s):660 - 669.

[2] Mayer, C.E.; Jaeger, B.E.; Crane, R.K.; Xuhe Wang; "Ka-band scintillations: measurements and model predictions"; Procs. of the IEEE Volume 85, Issue 6, June 1997 Page(s):936 - 945.

[3] Moulsley, T.; Vilar, E.; "Experimental and theoretical statistics of microwave amplitude scintillations on satellite down-links"; Antennas and Propagation, IEEE Transactions on [legacy, pre - 1988] Volume 30, Issue 6, Nov 1982 Page(s):1099 - 1106.

[4] Gremont, B.; Filip, M.; Gallois, P.; Bate, S.; "Comparative analysis and performance of two predictive fade detection schemes for Ka-band fade countermeasures"; Sel. Areas in Comm., IEEE Journal on Volume 17, Issue 2, Feb. 1999 Page(s):180 - 192.

[5] ESA/ESTEC project "Adaptive DVB-RCS1/DVB-S2 On-Board Processing (OBP) for Broadband Meshed Communications" (ARTES 4 Programme).

[6] Bede Liu; Munson, D., Jr.; "Generation of a random sequence having a jointly specified marginal distribution and autocovariance"; Acoustics, Speech, and Signal Processing, IEEE Transactions on Volume 30, Issue 6, Dec 1982 Page(s):973 - 983.

[7] Roquet Lloret, V.; Gimonet, E.; "Spectral characteristics of propagation impairments on experimental Earth-space links at Ka and V bands"; Castanet, L.; Antennas and Propagation, 2001. Eleventh International Conference on (IEE Conf. Publ. No. 480) Volume 2, 17-20 April 2001 Page(s):556 - 559 vol.2.

[8] Scharf, L.; "Statistical Signal Processing"; Prentice-Hall, 1990. ISBN-13: 978-0201190380.